NASA TECHNICAL NOTE

NASA TN D-6550

NASA TN D-6550

PREDICTION OF CENTERLINE SHOCK-LAYER THICKNESS AND PRESSURE DISTRIBUTION ON DELTA WING-BODY CONFIGURATIONS

by George E. Kaattari

Ames Research Center
Moffett Field, Calif. 94035

NATIONAL AERONAUTICS AND SPACE ADMINISTRATION • WASHINGTON, D. C. • OCTOBER 1971

1. Report No.	2. Government Accession No.	3. Recipi...
NASA TN D-6550		

4. Title and Subtitle	5. Report Date
PREDICTION OF CENTERLINE SHOCK-LAYER THICKNESS AND PRESSURE DISTRIBUTION ON DELTA WING-BODY CONFIGURATIONS	October 1971
	6. Performing Organization Code
7. Author(s)	8. Performing Organization Report No.
George E. Kaattari	A-4013
	10. Work Unit No.
9. Performing Organization Name and Address	124-07-28-01-00-21
NASA Ames Research Center Moffett Field, Calif. 94035	11. Contract or Grant No.
	13. Type of Report and Period Covered
12. Sponsoring Agency Name and Address	Technical Note
National Aeronautics and Space Administration Washington, D. C., 20546	14. Sponsoring Agency Code

15. Supplementary Notes

16. Abstract

Methods are presented to calculate both the shock inclination angle and the surface pressure coefficient in the vertical plane of symmetry of bodies at angle of attack. The methods are applicable over an angle-of-attack range from 0° to a maximum angle that depends on the body slenderness ratio; for very slender bodies, this maximum angle of attack approaches 90°. The methods apply to configurations of elliptical cross section and of rectangular cross section with rounded corners.

17. Key Words (Suggested by Author(s))	18. Distribution Statement
Cones Pressure distributions Shock-layer thickness Wing-body	Unclassified - Unlimited

19. Security Classif. (of this report)	20. Security Classif. (of this page)	21. No. of Pages	22. Price*
Unclassified	Unclassified	23	$3.00

*For sale by the National Technical Information Service, Springfield, Virginia 22151

NOTATION

a	semiminor axis of an ellipse
b	semimajor axis of an ellipse or semispan of a slab section
C_p	surface pressure coefficient
C_{p_θ}	pressure coefficient behind oblique shock inclined $\theta°$ with respect to free-stream direction
k	parameter defined by equation (3)
ℓ	length of cone
M_o	free-stream Mach number
m	virtual shock element (sketch (a))
n	element of actual shock
P	surface pressure on cone plane of symmetry
P_o	free-stream pressure
P_θ	pressure behind oblique shock inclined $\theta°$ to free-stream direction
q_o	free-stream dynamic pressure
r_c	corner radius of slab section
s	length along body surface from nose apex (fig. 3)
V_o	free-stream velocity
$\overline{V}_y$	average velocity normal to shock in shock layer
X	axis tangent to oblique shock (sketch (a))
x_o	cone base reference length in X-direction
Y	axis normal to oblique shock (sketch (a))
α	angle of attack
β	angle between shock and cone surface
γ	specific heat ratio of gas
Δ_o	shock standoff distance for yawed cylinders

Δ_s shock standoff distance on arbitrary body at location s

ΔP pressure increment between shock and yawed cylinder surface in plane of symmetry

Δx length increment of transformed body (sketch (a))

ε_y semiapex angle of cone in minor axis plane

ε_z semiapex angle of cone in major axis plane

θ inclination angle of shock to free-stream direction

ρ_o free-stream gas density

ρ_θ gas density behind oblique shock inclined $\theta°$ to free-stream direction

PREDICTION OF CENTERLINE SHOCK-LAYER THICKNESS AND PRESSURE DISTRIBUTION ON DELTA WING-BODY CONFIGURATIONS

George E. Kaattari

Ames Research Center

SUMMARY

Methods are presented to calculate both the shock inclination angle and the surface pressure coefficient in the vertical plane of symmetry of bodies at angle of attack. The methods are applicable over an angle-of-attack range from 0° to a maximum angle that depends on the body slenderness ratio; for very slender bodies, this maximum angle of attack approaches 90°. The methods apply to configurations of elliptical cross section and of rectangular cross section with rounded corners.

INTRODUCTION

There is much interest currently in pressures and shock-layer thicknesses generated on bodies at large angles of attack during atmosphere entry. Theoretical solutions (refs. 1 and 2) have been developed for pressure distributions and shock-layer thicknesses for symmetrical profiles at zero angle of attack. A recent work that uses numerical solutions of exact equations (ref. 3) has considered the case of nonsymmetric bodies at angle of attack. Approximate pressure distributions have been computed for more general (nonanalytic) shapes such as wing-body combinations by tangent wedge and tangent circular cone methods and by Newtonian theory.

The present method of estimating the shock locations and surface pressure coefficients in the vertical plane of symmetry is based on analysis of a simple cone at angle of attack. The method may be extended, however, to the prediction of symmetry plane pressures and shock-layer thicknesses of configurations with arbitrarily varying (and expanding) cross sections. This extension to the method is accomplished by approximation of the body with a tandem series of cone frustums of appropriate cross section. In effect, this then is a tangent cone method but differs from the standard technique in that the tangent cone can be made to coincide closely with the entire windward local body periphery in the spanwise direction. This requirement is not possible with a circular cone that can be tangent only to a point on the body and thus cannot give a realistic shock-layer thickness. The present method, moreover, is more applicable to a larger angle-of-attack range than is the method of the tangent circular cone.

ANALYSIS

The analysis will be developed in two parts. The first part will discuss a semiempirical equation used to calculate the pressure coefficient in the vertical plane of symmetry on a conical body of arbitrary cross section at angle of attack. The equation is a function of the free-stream flow properties, the shock inclination angle, θ, and the differential angle, β, between the shock trace and the body surface in the vertical plane of symmetry. The second part presents a means of calculating the angle, β, as a function of angle of attack, α, for conical bodies having two types of body cross section.

Pressure Coefficient

The pressure coefficient for a perfect gas behind an oblique shock at angle θ is

$$\frac{P_\theta - P_o}{q_o} = C_{p_\theta} = \frac{4}{(\gamma+1)}\left(\sin^2\theta - \frac{1}{M_o^2}\right) \tag{1}$$

When the oblique shock is associated with a wedge (two-dimensional flow), the angle between the wedge and shock is $\beta = \tan^{-1}[(\rho_o/\rho_\theta)\tan\theta]$, where ρ_o/ρ_θ is the reciprocal shock density ratio across the oblique shock. The pressure coefficient on the wedge is identical to C_{p_θ} (eq. (1)). If the shock is associated with an infinitely long ($\varepsilon_y = 0$) yawed cylinder, the shock trace is parallel to the cylinder and $\beta = 0°$. The pressure coefficient on the cylinder is then due to the stagnation pressure corresponding to the normal Mach number $M_o \sin\theta$. The increase in pressure coefficient from the shock to the cylinder surface may be determined with the aid of shock tables. For normal Mach numbers, greater than 2.5, this increase is given to a good approximation (within 6 percent) by

$$\frac{\Delta P}{q_o} = \frac{\rho_o}{\rho_\theta}\sin^2\theta = \frac{\gamma-1}{\gamma+1}\sin^2\theta + \frac{2}{(\gamma+1)M_o^2} \tag{2}$$

It is assumed that the variation in the surface pressure coefficient between the limiting cases of a wedge and a yawed cylinder is a linear function of the parameter k defined by

$$k = \frac{\tan\beta}{(\rho_o/\rho_\theta)\tan\theta} \tag{3}$$

The "generalized" pressure coefficient is then

$$C_p = C_{p_\theta} + \frac{\Delta P}{q_o}(1 - k) \tag{4}$$

Equations (1), (2), and (3) when combined with equation (4) result in

$$C_p = \frac{(\gamma+3)}{(\gamma+1)} \sin^2 \theta - \frac{2}{(\gamma+1)M_o^2} - \sin \theta \cos \theta \tan \beta \qquad (5)$$

When applied to elliptic cones at angle of attack, equation (5) was found to agree well with the results of a more rigorous analysis developed in reference 4 (see fig. 1). The centerline pressures given by the present method were also found to agree substantially with the values given by a semi-empirical technique presented in reference 5.

Shock and Body Angle Relationships

Equation (5) presumes a known relationship between the angles θ and β. This relationship is not generally available from existing theories for conical bodies of arbitrary cross section at angle of attack. This section, therefore, describes a method by which the shock and body angle relationships may be determined by simple calculations involving two-dimensional shock theory.

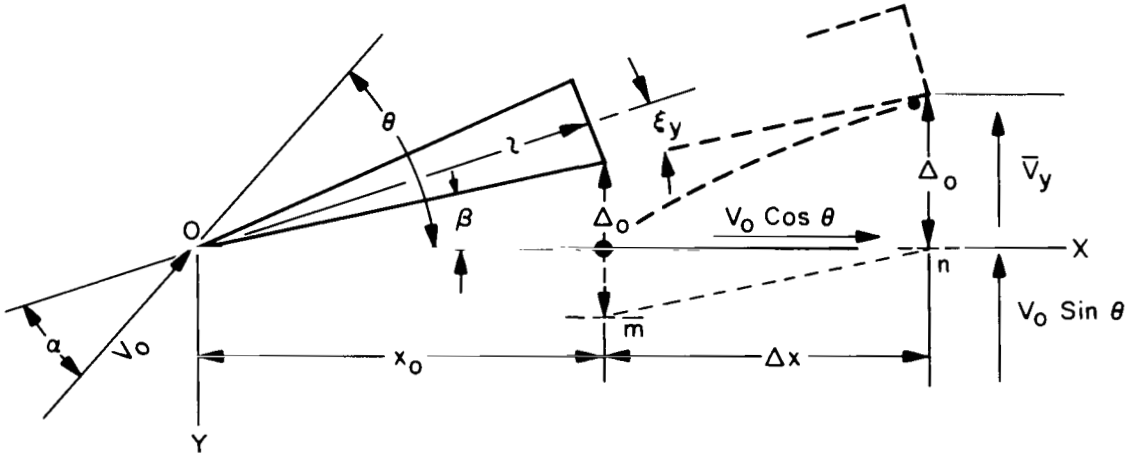

Sketch (a)

Sketch (a) depicts a conical body with its upper surface element in the vertical plane of symmetry defining an angle β with respect to the shock trace OX, which is inclined at the angle θ with respect to the free-stream direction. If the horizontal component of velocity, $V_o \cos \theta$, is neglected, the shock standoff distance Δ_o from the base of the body at location x_o to a "virtual" shock location, element m, is established by two-dimensional shock applied to the local body cross section in the normal flow field. When the horizontal component of velocity is considered, the standoff distance Δ_o is maintained with respect to an extension of the body surface element but is translated a distance Δx, so that the virtual shock element m appears at the real location n on the shock trace OX, this position being occupied

with respect to a transformed (elongated) body. Since the value, Δ_o, is established, β may be determined by the following procedure using the length of the transformed body $x_o+\Delta x$.

The Y-components of the stream velocity in the shock layer varies from the value immediately behind the shock, $(\rho_o/\rho_\theta)V_o \sin\theta$, to the value approaching the body surface, $V_o \cos\theta \tan\beta$. The average velocity $\overline{V}_y = (1/2)V_o[(\rho_o/\rho_\theta)\sin\theta + \cos\theta \tan\beta]$. The X-component of velocity is $V_o \cos\theta$. Therefore, a stream particle commencing from the shock at x_o is carried the horizontal distance Δx with velocity $V_o \cos\theta$ in the time interval required for it to approach the transformed body at Y-distance Δ_o with the average velocity $\overline{V}_y$. Thus

$$\frac{\Delta_o}{\Delta x} = \frac{\overline{V}_y}{V_o \cos\theta} = \frac{1}{2}\left(\frac{\rho_o}{\rho_\theta}\tan\theta + \tan\beta\right) \tag{6}$$

From sketch (a)

$$\Delta_o - x_o \tan\beta = \Delta x \tan\beta \tag{7}$$

Substitution of equation (7) into equation (6) gives

$$\tan\beta\left(\tan\beta + \frac{\rho_o}{\rho_\theta}\tan\theta\right) + \frac{\Delta_o}{x_o}\left(\tan\beta - \frac{\rho_o}{\rho_\theta}\tan\theta\right) = 0 \tag{8}$$

in which x_o is related to the cone geometry by

$$\left.\begin{aligned} &\frac{\ell}{\cos\varepsilon_y} = \frac{x_o}{\cos\beta}\,, \quad b = \ell\tan\varepsilon_z\,, \quad a = \ell\tan\varepsilon_y \\ &\frac{1}{x_o} = \frac{\tan\varepsilon_z \cos\varepsilon_y \sec\beta}{b} \end{aligned}\right\} \tag{9}$$

Substitution of the above value for x_o into equation (8) gives the final result

$$\tan\beta\left(\tan\beta + \frac{\rho_o}{\rho_\theta}\tan\theta\right) + \frac{\Delta_o \tan\varepsilon_z \cos\varepsilon_y \sec\beta}{b}\left(\tan\beta - \frac{\rho_o}{\rho_\theta}\tan\theta\right) = 0 \tag{10}$$

Equation (10) gives β as a function of θ; however, β as a function of angle of attack α is readily found through the relationship $\alpha = \theta - \beta - \varepsilon_y$ (sketch (a)).

The useful angle-of-attack range of the method is restricted in that when the centerline shock-trace incline approaches $\theta = 90°$, the angle β approaches the approximate value $(\Delta_o/b)\varepsilon_z$. The limiting angle of attack is then $\alpha \approx 90° - (\Delta_o/b)\varepsilon_z - \varepsilon_y$. Thus, α reaches the highest value for slender cones (small ε_z and ε_y), and for cones of a given slenderness, has higher values with increasing Mach number (decreasing Δ_o/b).

For small values of β (sec $\beta = 1$), equation (10) can be formed as a quadratic equation and an approximate solution readily obtained. The exact solution in chart form is presented in figure 2, wherein β is plotted as a function of $(\Delta_o/b)\tan \varepsilon_z \cos \varepsilon_y$ for various parameter values $(\rho_o/\rho_\theta)\tan \theta$. The required value Δ_o/b is the shock solution for two-dimensional cylinders and is a function of the shock-density ratio and the body cross section. Solutions for various elliptic cross sections and slab sections with round corners are given in figure 3. These solutions are from an unpublished method that is a two-dimensional extension to the axisymmetric solutions of reference 6. The discontinuities in the solutions are due to arbitrary step changes in the value of the gas specific-heat ratio, γ, at $\rho_\theta/\rho_o = 6$ and 11. The effect of γ may be estimated by interpolation if some "real gas" γ can be specified.

EXAMPLE APPLICATION

The following numerical example illustrates the calculative procedure and use of the charts herein to determine the shock angle and pressure-coefficient solutions for a typical conical body at an angle of attack in air ($\gamma = 1.4$) at Mach number 5.

Given $a/b = 1/3$, $\varepsilon_z = 15°$ ($\varepsilon_y = 5.10°$), and $M_o = 5$, determine the angle of attack and pressure coefficient when the shock is inclined ($\theta = 60°$) to the free stream. The shock-density ratio, ρ_o/ρ_θ, across the oblique shock with $\gamma = 1.4$ is first determined:

$$\frac{\rho_o}{\rho_\theta} = \frac{(\gamma-1)}{(\gamma+1)} + \frac{2}{(\gamma+1)M_o^2 \sin^2 \theta} = \frac{0.4}{2.4} + \frac{2}{2.4 \times 25 \times 0.750} = 0.211$$

The reciprocal value, $\rho_\theta/\rho_o = 4.74$. In figure 3(a), $\Delta_o/b = 0.692$ at $\rho_\theta/\rho_o = 4.74$ for an elliptic section with $a/b = 1/3$.

Quantities required in figure 2 are now evaluated. The abscissa value $(\Delta_o/b)\tan \varepsilon_z \cos \varepsilon_y = 0.692 \times 0.268 \times 0.996 = 0.185$. The parameter

$$(\rho_o/\rho_\theta)\tan \theta = 0.211 \times 1.732 = 0.366$$

The above values intersect on the curves of figure 2(a) at the ordinate value $\beta = 5.85°$. The angle of attack

$$\alpha = \theta - \beta - \varepsilon_y = 60° - 5.85° - 5.10° = 49.05°$$

The pressure coefficient (eq. (5)) is evaluated

$$C_p = \frac{4.4}{2.4} \times 0.750 - \frac{2}{2.4 \times 25} - 0.500 \times 0.866 \times 0.1025 = 1.297$$

Note that a specific angle-of-attack value cannot be selected *a priori*. Calculations with several values of θ can be made quickly, however, and curves of C_p and β constructed as functions of angle of attack. The above procedure also applies to round-corner slab sections where r_c takes the role of "a" (fig. 3(b)).

EXTENSION OF THE METHOD

A delta wing-body configuration is depicted by solid outline in figure 3. The dashed lines represent outlines of a series of tandem cone frustums with which the configuration shape is approximated. The cone elements are constructed tangent to the bottom surface at the vertical plane of symmetry and are also made tangent to the planform outline of the configuration as indicated. A typical cross section meeting these requirements is shown. Cross sections varying from a circle to ellipses of increasing ellipticity and several round-corner slab sections were used in the construction of figure 4. Thus, the actual configuration is approximated by a series of cone frustums of stepwise varying cross section, apex angle, and angle of attack. The accuracy of the approximation increases with the number of frustums used.

Calculations of pressures and shock angles are then made for the individual cones in the manner of the above example calculation. The shock-layer thickness is then determined by integration of the local shock angles (appropriate to each cone) plotted as a function of body surface length:

$$\Delta_s = \int_0^s \beta \, ds = \int_0^s (d\Delta/ds) ds \tag{11}$$

Equation (11) may be integrated by either graphical or tabular methods.

COMPARISON BETWEEN EXPERIMENTAL AND THEORETICAL RESULTS

Cones

Comparisons of experimental and predicted results of β as a function of α for elliptic cones are presented in figure 5. A wide range in cone geometry and Mach number ($3 < M_o < 10$) is represented. Agreement between experimental and predicted values is generally within 10 percent and is

particularly satisfactory at the higher Mach numbers. The data at Mach numbers 2.94, 3.87, and 4.78 are previously unpublished results of tests in the Ames 1- by 3-Foot Wind Tunnel.

A comparison between experimental and predicted centerline pressures for cones is presented in figure 6 in the form of a correlation curve. The ranges of angles of attack, Mach numbers, and configuration cross sections are noted on the figure. Experimental and predicted values correlate within the limits of about ±2 percent.

Wing-Body

A comparison between experimental and predicted centerline shock-layer thickness for a delta wing-body configuration at $M_0 = 7.4$ is shown in figure 7. Experimental and predicted values agree well. Note that the shock-layer thickness has the same value at $\alpha = 15°$ and 30°.

Figure 8 presents a comparison between experimental and predicted centerline pressure distributions for the delta-wing and body configuration shown in figure 7. Agreement is satisfactory at angles of attack up to 30°. At $\alpha = 40°$ a discrepancy between experimental and predicted pressures occurs over a portion of the body length; however, the predicted values given by the present method are in better accord with experiment than are the indicated results of modified Newtonian theory.

CONCLUDING REMARKS

Simple methods were developed for prediction of inclination of a shock with respect to the windward trace on a conical surface in the vertical plane of symmetry and for estimation of pressure coefficient on this body trace.

Predicted values were compared with experiments for air flows in the Mach number range 3 to 10 and the angle-of-attack range of 0° to about 70° for cones of a wide range in geometry. The methods were extended to the prediction of vertical symmetry plane shock-layer thicknesses and body surface pressures of configurations with arbitrarily changing cross sections with body length by the use of a tandem series of locally conical elements to approximate the body shape. This, in effect, is a refined tangent cone procedure.

The applicability of the methods has been demonstrated by comparison with test results from low enthalpy air flows. The suitability of the method for real gas flows is believed valid also since the real gas effect enters primarily through the density ratio across the shock.

Ames Research Center
National Aeronautics and Space Administration
Moffett Field, Calif., 94035, July 8, 1971

REFERENCES

1. Van Dyke, Milton D.; and Gordon, Helen D.: Supersonic Flow Past a Family of Blunt Axisymmetric Bodies. NASA TR R-1, 1959.

2. Fuller, Franklyn B.: Numerical Solutions for Supersonic Flow of an Ideal Gas Around Blunt Two-Dimensional Bodies. NASA TN D-791, 1961.

3. Rakich, John V.: A Method of Characteristics for Steady Three-Dimensional Supersonic Flow with Application to Inclined Bodies of Revolution. NASA TN D-5341, 1969.

4. Cleary, Joseph W.: Approximation for Distribution of Flow Properties in the Angle-of-Attack Plane of Conical Flows. NASA TN D-5951, 1970.

5. Kaattari, George E.: A Method for Predicting Pressures on Elliptic Cones at Supersonic Speeds. NASA TN D-5952, 1970.

6. Kaattari, George E.: A Method for Predicting Shock Shapes and Pressure Distributions for a Wide Variety of Blunt Bodies at Zero Angle of Attack. NASA TN D-4539, 1968.

7. Palko, R. L.; and Ray, A. D.: Pressure Distribution and Flow Visualization Tests of a 1.5 Elliptic Cone at Mach 10. Rep. AEDC-TDR-63-163, 1963.

8. Randall, R. E.; Bell, D. R.; and Burk, J. L.: Pressure Distribution Tests of Several Sharp Leading Edge Wings, Bodies, and Body-Wing Combinations at Mach 5 and 8. AEDC-TN-60-173, 1960.

9. Bernot, Peter T.: Pressure Distributions on Blunt Delta Wings at Angles of Attack Up to 90° and Mach Number of 6.85. NASA TN D-1954, 1963.

10. Squire, L. C.: Pressure Distributions and Flow Patterns at M = 4.0 on Some Delta Wings. ARC R & M No. 3373, Ministry of Aviation, 1964.

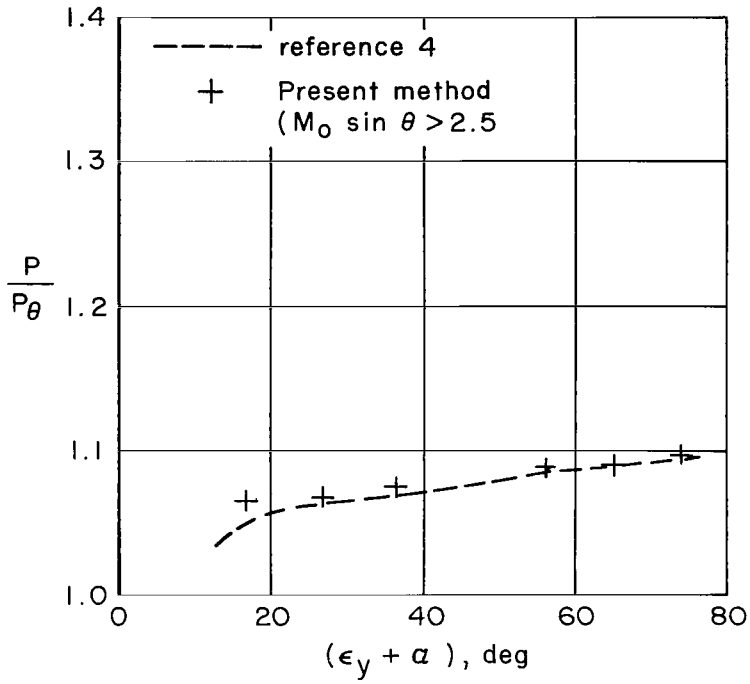

Figure 1.- Comparison of cone surface-pressure ratio given by the present method and that of reference 5, $M_0 = 10$, $a/b = 2/3$, $\epsilon_y = 15.2°$.

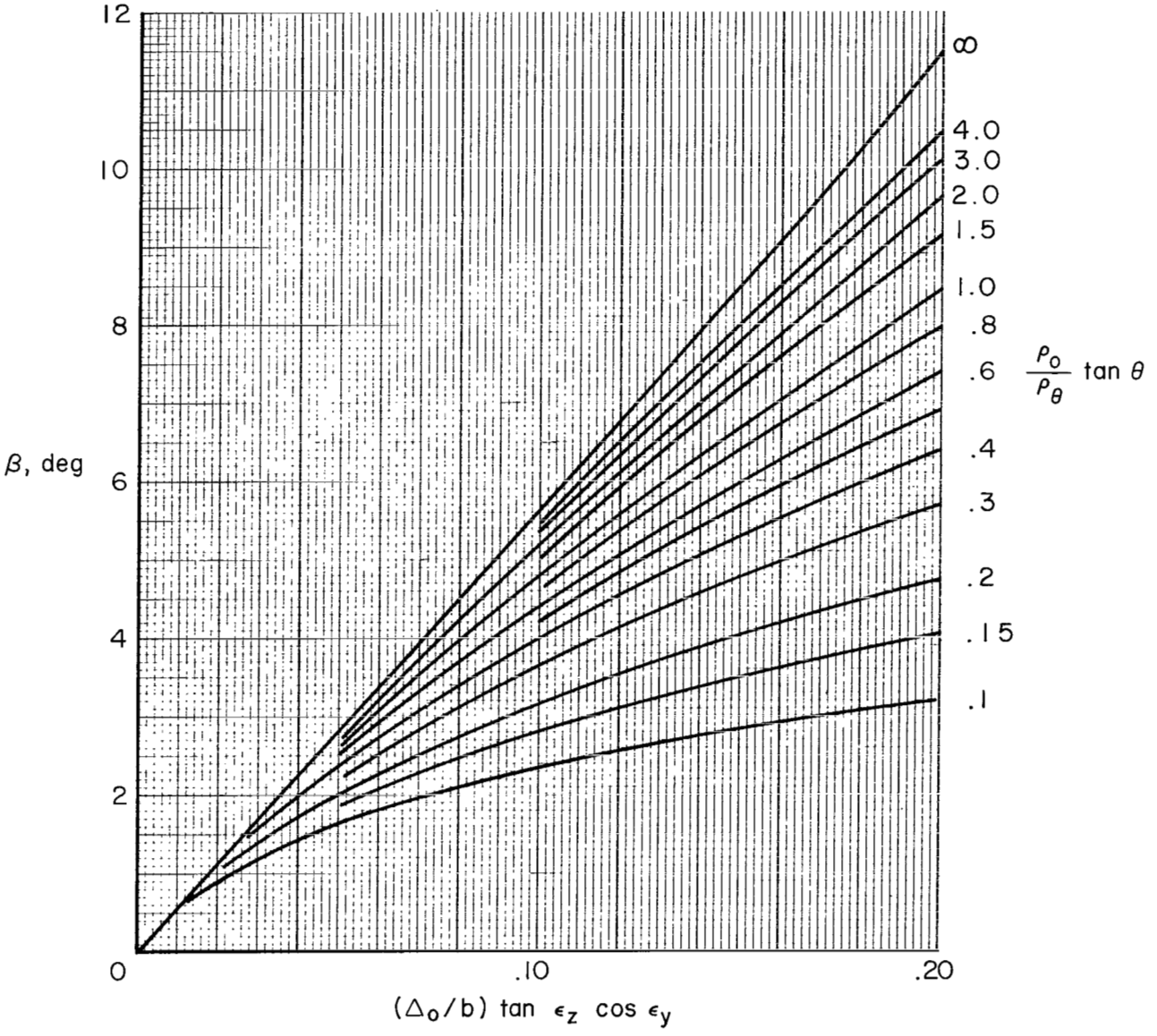

(a) $(\Delta_0/b)\tan \varepsilon_z \cos \varepsilon_y = 0$ to 0.20

Figure 2.- Solutions of equation (10) for the angle β.

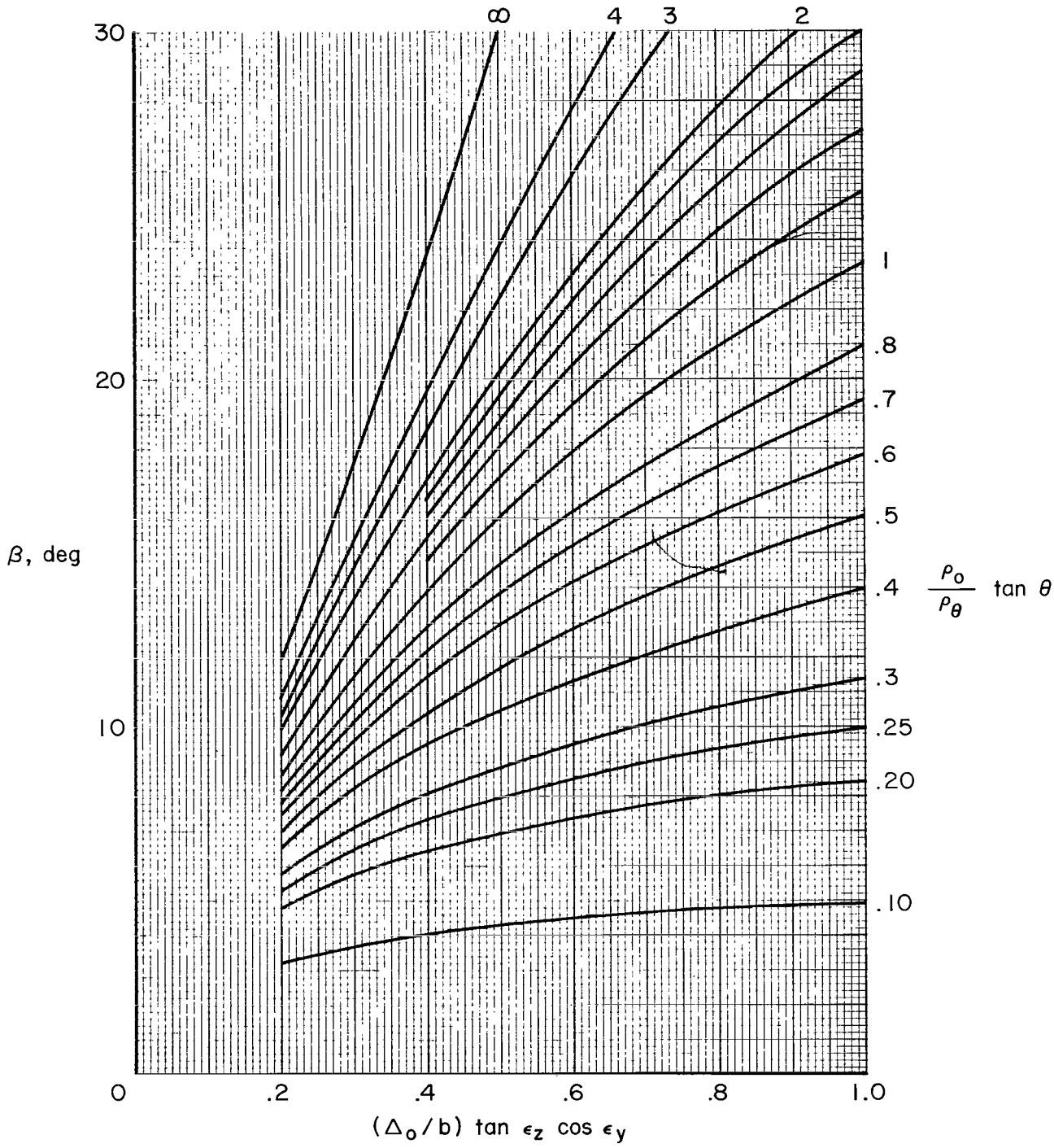

(b) $(\Delta_0/b)\tan \varepsilon_z \cos \varepsilon_y = 0.2$ to 1.0

Figure 2.- Concluded.

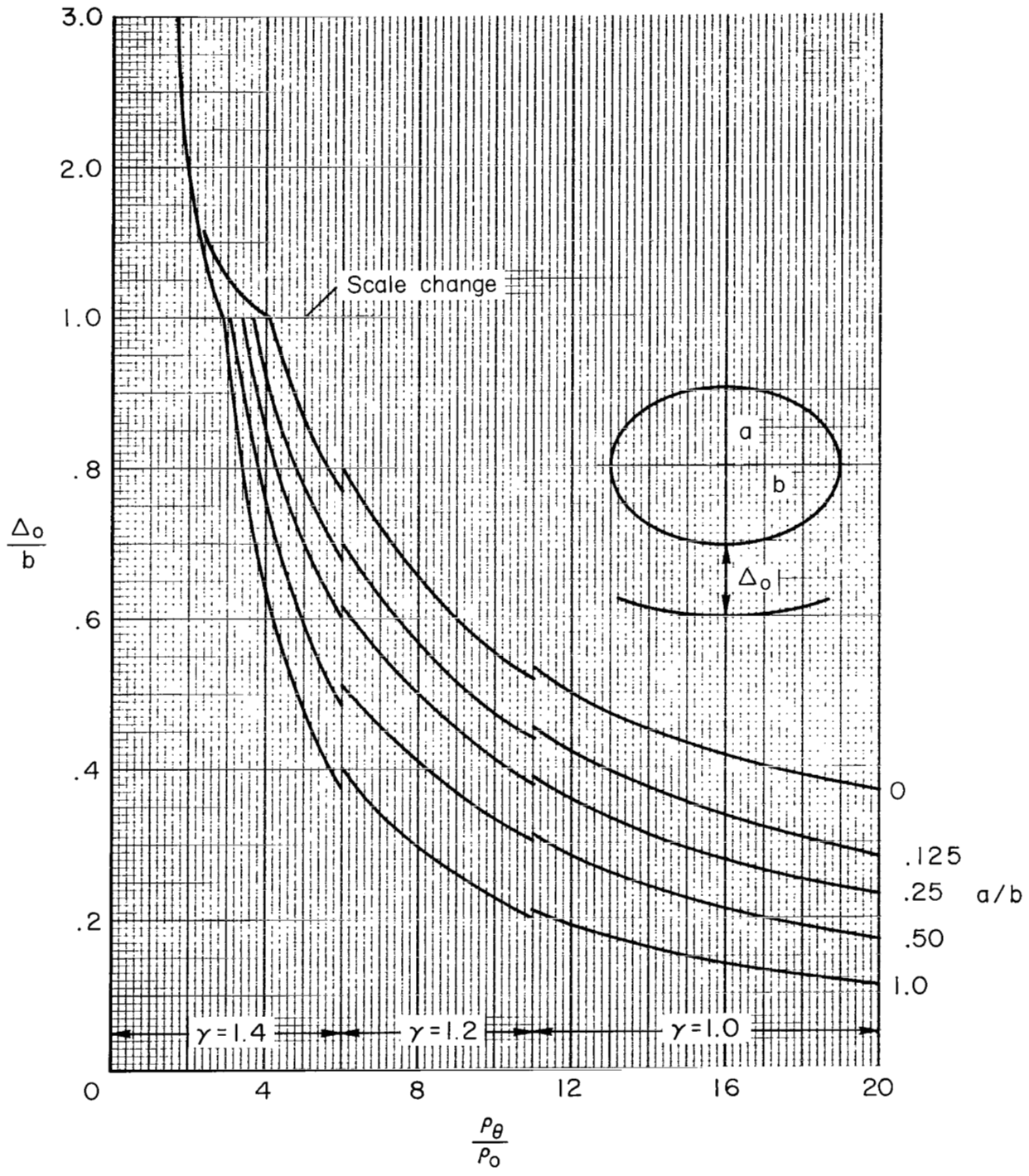

(a) Elliptic cylinder sections.

Figure 3.- Centerline shock standoff.

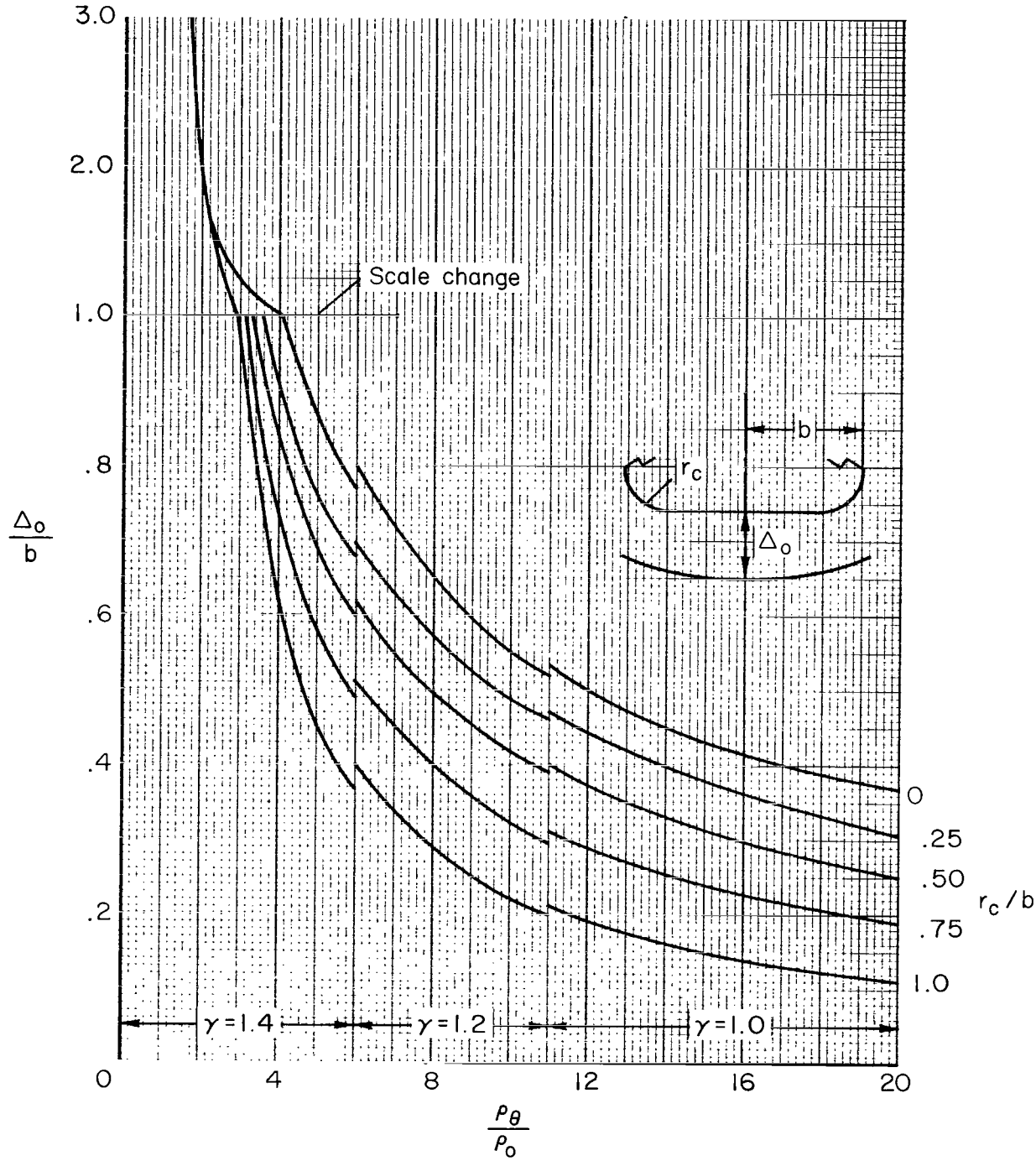

(b) Round-corner slab sections.

Figure 3.- Concluded.

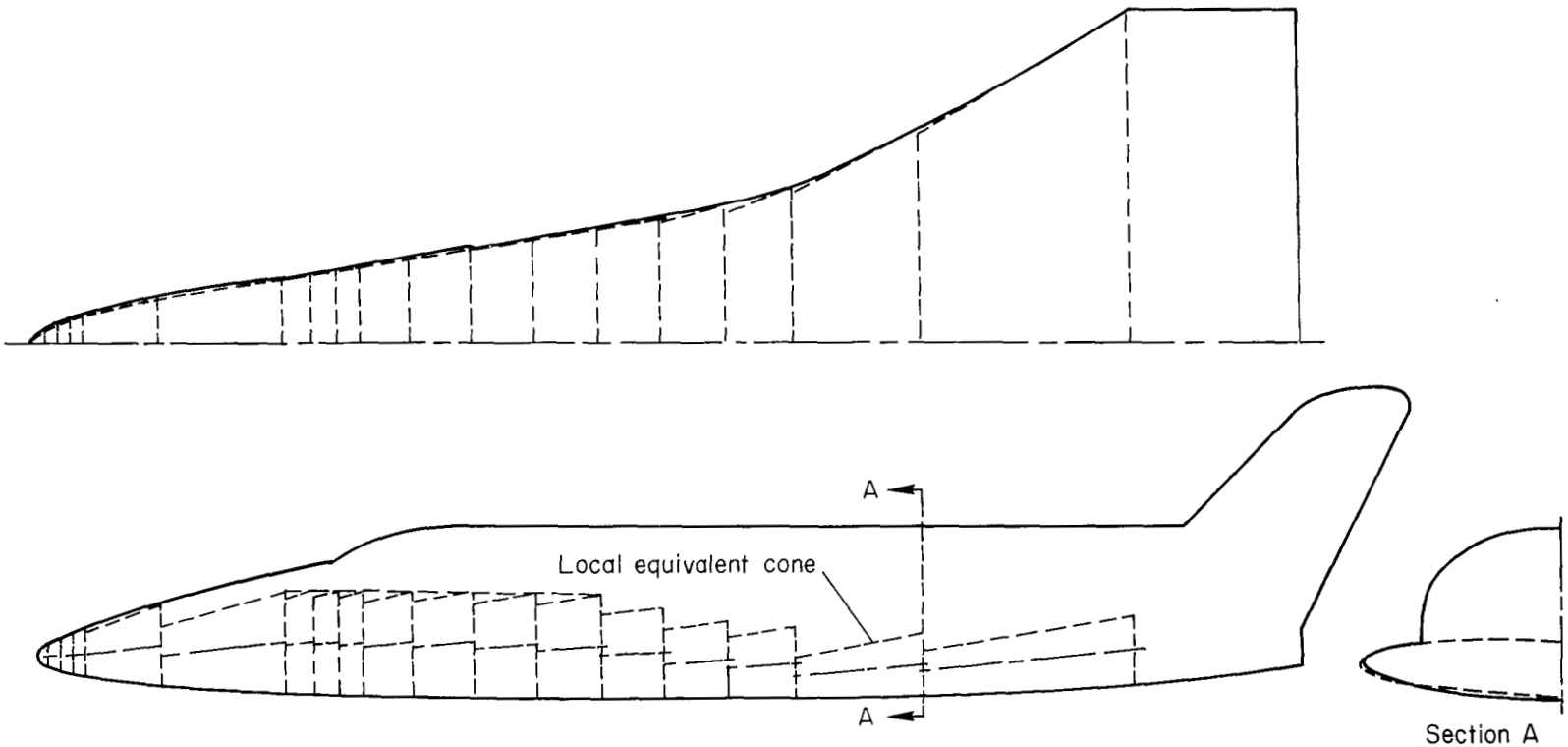

Figure 4.- Approximation of delta-wing-body by cone frustums.

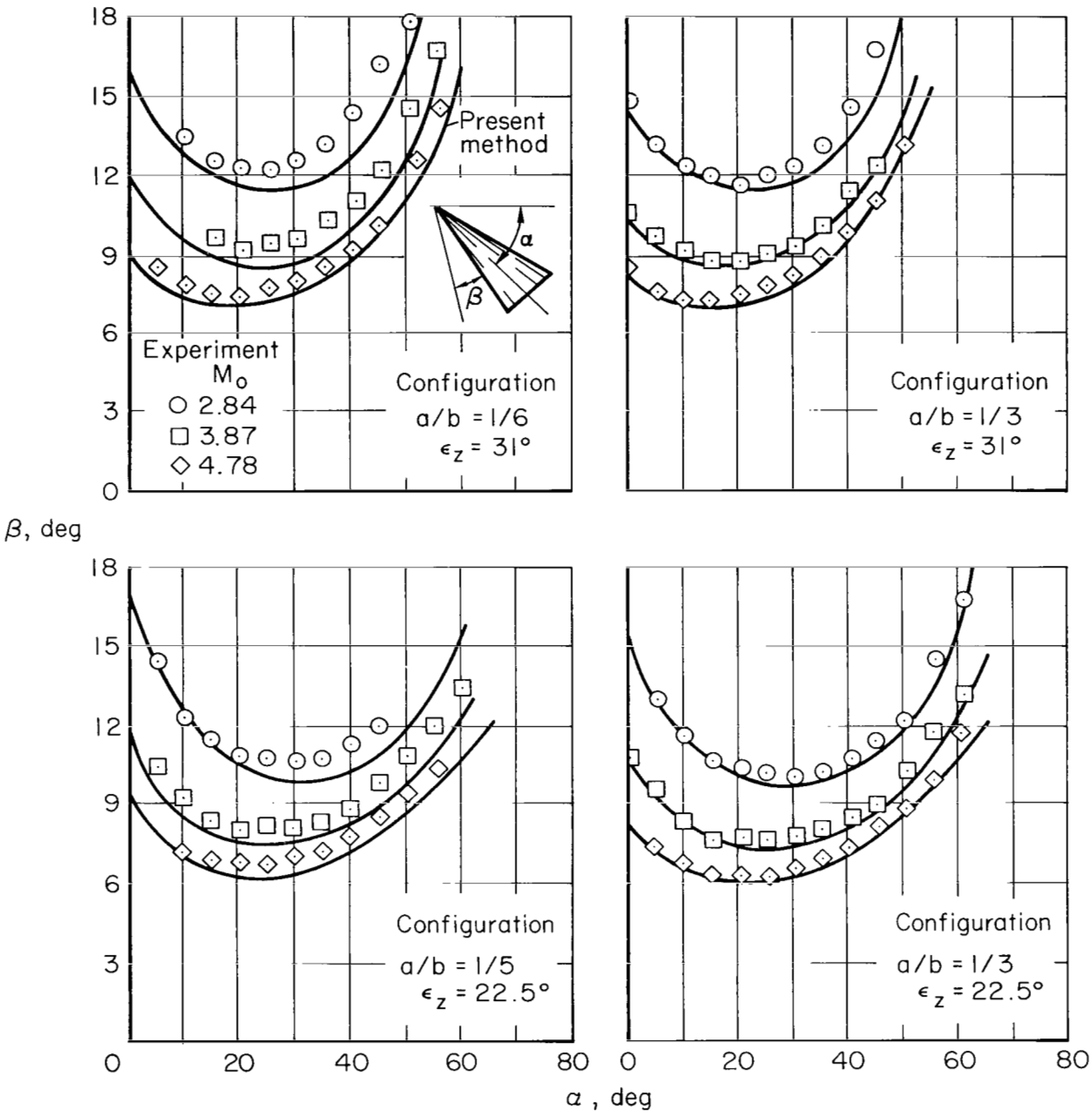

Figure 5.- Experimental and predicted values of β as a function of angle of attack, α.

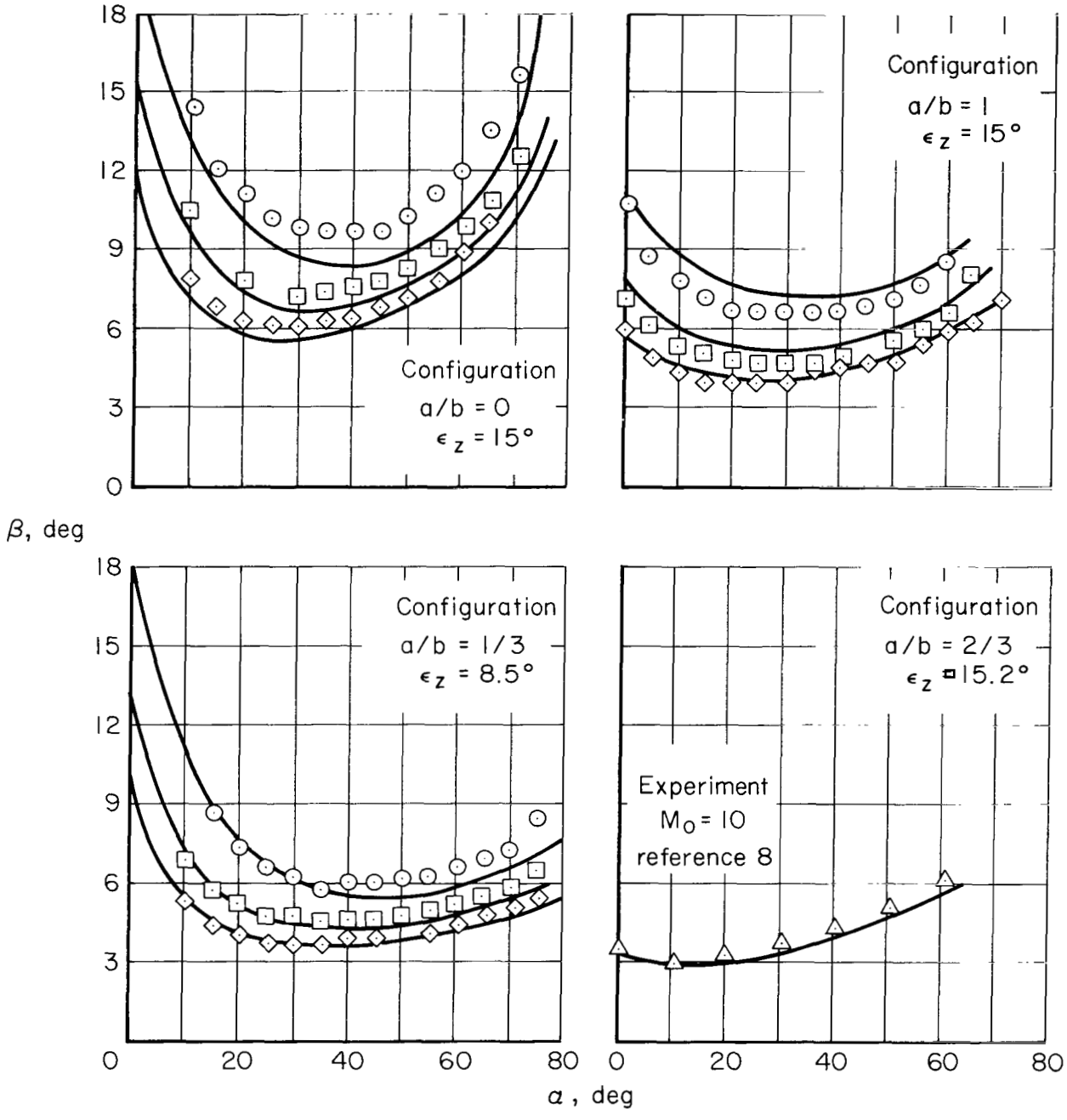

Figure 5.- Concluded.

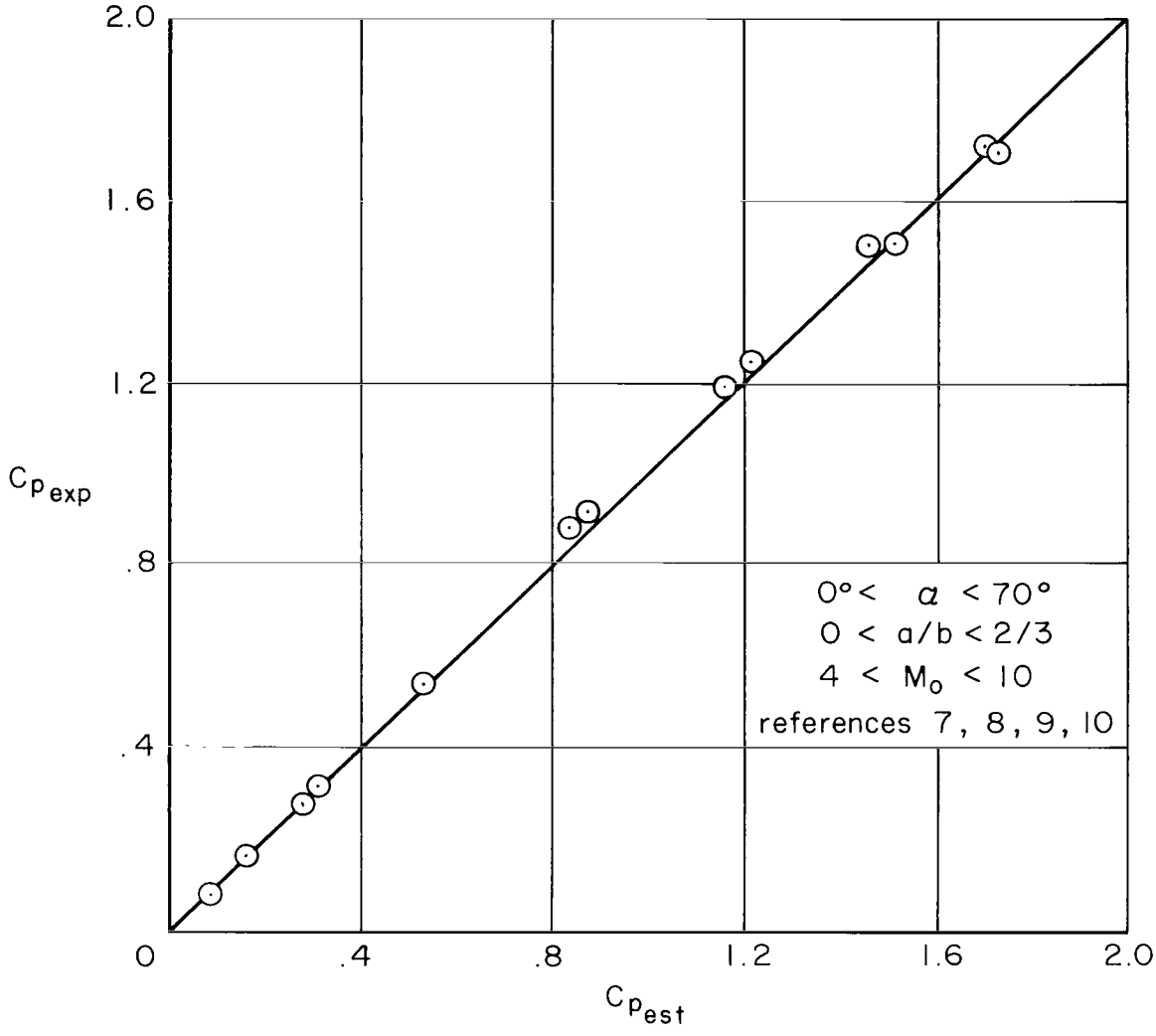

Figure 6.- Correlation of experimental and predicted centerline pressure coefficients on cones.

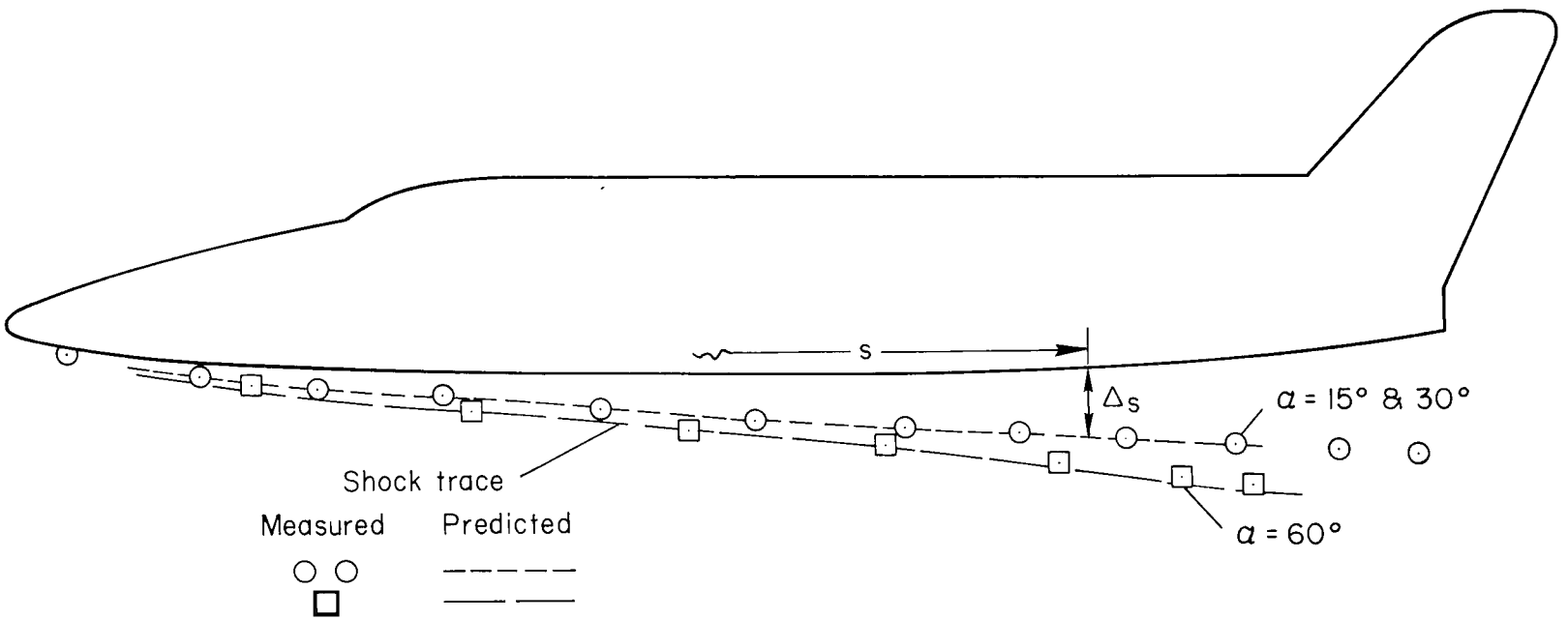

Figure 7.- Comparison of measured and predicted centerline shock-layer thickness on delta-wing-body; $M_0 = 7.4$.

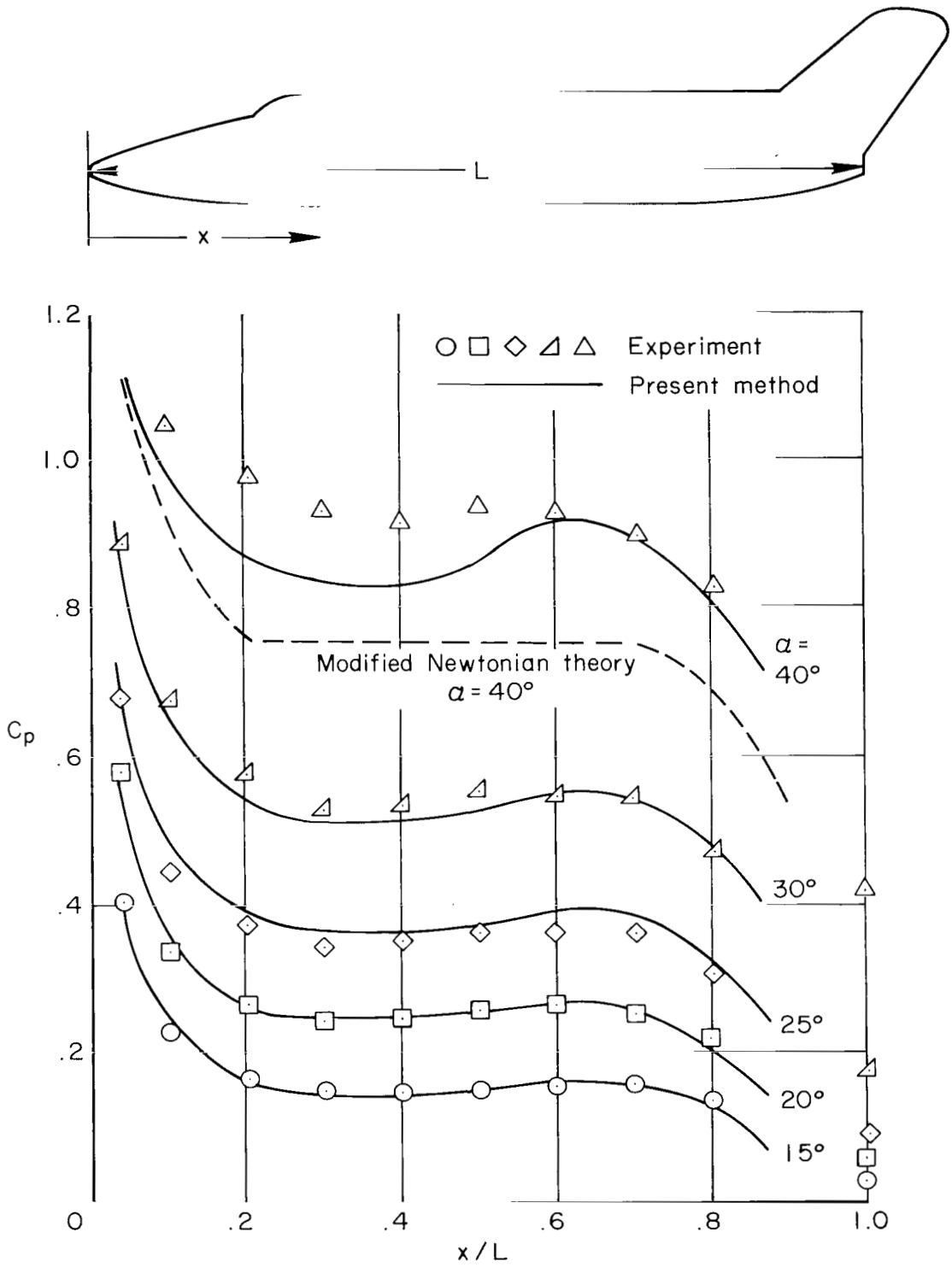

Figure 8.- Experimental and predicted pressure distributions on delta-wing-body configuration; $M_0 = 7.4$.

"The aeronautical and space activities of the United States shall be conducted so as to contribute . . . to the expansion of human knowledge of phenomena in the atmosphere and space. The Administration shall provide for the widest practicable and appropriate dissemination of information concerning its activities and the results thereof."

—NATIONAL AERONAUTICS AND SPACE ACT OF 1958

NASA SCIENTIFIC AND TECHNICAL PUBLICATIONS

TECHNICAL REPORTS: Scientific and technical information considered important, complete, and a lasting contribution to existing knowledge.

TECHNICAL NOTES: Information less broad in scope but nevertheless of importance as a contribution to existing knowledge.

TECHNICAL MEMORANDUMS: Information receiving limited distribution because of preliminary data, security classification, or other reasons.

CONTRACTOR REPORTS: Scientific and technical information generated under a NASA contract or grant and considered an important contribution to existing knowledge.

TECHNICAL TRANSLATIONS: Information published in a foreign language considered to merit NASA distribution in English.

SPECIAL PUBLICATIONS: Information derived from or of value to NASA activities. Publications include conference proceedings, monographs, data compilations, handbooks, sourcebooks, and special bibliographies.

TECHNOLOGY UTILIZATION PUBLICATIONS: Information on technology used by NASA that may be of particular interest in commercial and other non-aerospace applications. Publications include Tech Briefs, Technology Utilization Reports and Technology Surveys.

Details on the availability of these publications may be obtained from:

SCIENTIFIC AND TECHNICAL INFORMATION OFFICE

NATIONAL AERONAUTICS AND SPACE ADMINISTRATION

Washington, D.C. 20546